Bioorg. Med. Chem. Lett. 41 (2021) 127983

Contents lists available at ScienceDirect

Bioorganic & Medicinal Chemistry Letters

journal homepage: www.elsevier.com/locate/bmcl

Discovery of a novel highly potent broad-spectrum heterocyclic chemical series of arenavirus cell entry inhibitors

Michael B. Plewe [a,†], Vidyasagar Reddy Gantla [a], Nadezda V. Sokolova [a], Young-Jun Shin [a], Shibani Naik [a], Eric R. Brown [a], Alexandra Fetsko [a], Lihong Zhang [b], Birte Kalveram [b], Alexander N. Freiberg [b], Greg Henkel [a], Ken McCormack [a,*]

[a] Arisan Therapeutics, 11189 Sorrento Valley Rd, Suite 104, San Diego 92121, CA, United States
[b] Department of Pathology, and Center for Biodefense and Emerging Infectious Diseases, The University of Texas Medical Branch, Galveston 77555, TX, United States

ARTICLE INFO

Keywords:
Arenavirus
Lassa
Junin
Machupo
Entry inhibitor

ABSTRACT

We identified and explored the structure–activity relationship (SAR) of a novel heterocyclic chemical series of arenavirus cell entry inhibitors. Optimized lead compounds, including diphenyl-substituted imidazo[1,2-*a*]pyridines, benzimidazoles, and benzotriazoles exhibited low to sub-nanomolar potency against both pseudotyped and infectious Old and New World arenaviruses, attractive metabolic stability in human and most nonhuman liver microsomes as well as a lack of hERG K + channel or CYP enzyme inhibition. Moreover, the straightforward synthesis of several lead compounds (e.g., the simple high yield 3-step synthesis of imidazo[1,2-*a*]pyridine **37**) could provide a cost-effective broad-spectrum arenavirus therapeutic that may help to minimize the cost-prohibitive burdens associated with treatments for emerging viruses in economically challenged geographical settings.

Arenaviruses represent a family of bisegmented ambisense RNA viruses comprised of a large number of species, a number of which are associated with acute hemorrhagic fevers (HF) in humans.[1–3] HF arenaviruses, including the Old World species Lassa (LASV) and the New World species Machupo (MACV) and Junin (JUNV), represent serious public health risks, especially in endemic regions of Africa and South America.[4–6] LASV presents the greatest current arenavirus-associated unmet global health need. Each year LASV is responsible for an estimated 300,000 human disease cases and 5000 deaths in Western Africa.[7–9] Mortality rates for hospitalized LASV HF patients are 15–20% and survivors often suffer permanent sequelae including bilateral hearing damage.[10–13] The nonspecific antiviral ribavirin currently offers the sole therapeutic option despite a lack of definitive clinical data to support its effectiveness and the risk of potentially serious adverse effects including thrombocytopenia and anemia.[14–17] Due to the high mortality rates and limited therapeutic options the development of potent, cost-effective and readily manufacturable at scale broad-spectrum arenavirus therapeutic agents to treat Lassa and other arenavirus hemorrhagic fevers is urgently needed.

Previously, we reported the SAR and optimization of a 4-acyl-1,6-dialkylpiperazin-2-one chemical series exhibiting potent broad-spectrum arenavirus activity (EC_{50} values < 10 nM) against vesicular stomatitis virus (VSV) pseudotyped viruses expressing Lassa (pLASV), Machupo (pMACV) or Junin (pJUNV) glycoproteins but only moderate *in vitro* liver microsome metabolic stability.[18] In further pursuit of identifying additional chemical series with potent broad-spectrum arenavirus activity and improved drug-like properties we initiated pharmacophore modeling of the piperazinone series with a previously reported 1,5-substituted benzimidazole chemical series, both of which have been reported to share an overlapping binding site in the arenavirus GP2 subunit and are resistant to the same attenuating resistance mutation unit (F427I) of the Candid#1 JUNV strain.[18–25] We initially noted that the piperazinone ARN-73594 (compound 35 in reference 18) shared similar groups at each end of the molecule (N^4 indole 5-methoxy group and the 3-methoxy group of the N^1 substituent) with that of the 1,5-substituted benzimidazole ST-37[19] and that in some conformations a carbonyl group essential for ARN-73594 activity displayed close overlap with N^3 of ST-37's 1-aryl-5-benzylamino benzimidazole core (Fig. 1, top panel). Subsequent 3D minimizations between the 3 atom pairs of ARN-73594 and ST-37 further provided coincident overlap (Fig. 1, bottom

* Corresponding author.
E-mail address: kenm@arisanthera.com (K. McCormack).
† Present address: Cullgen (USA) Inc., 12671 High Bluff Drive, Suite 130, San Diego, CA 92130, United States.

https://doi.org/10.1016/j.bmcl.2021.127983
Received 23 December 2020; Received in revised form 12 March 2021; Accepted 14 March 2021
Available online 5 May 2021

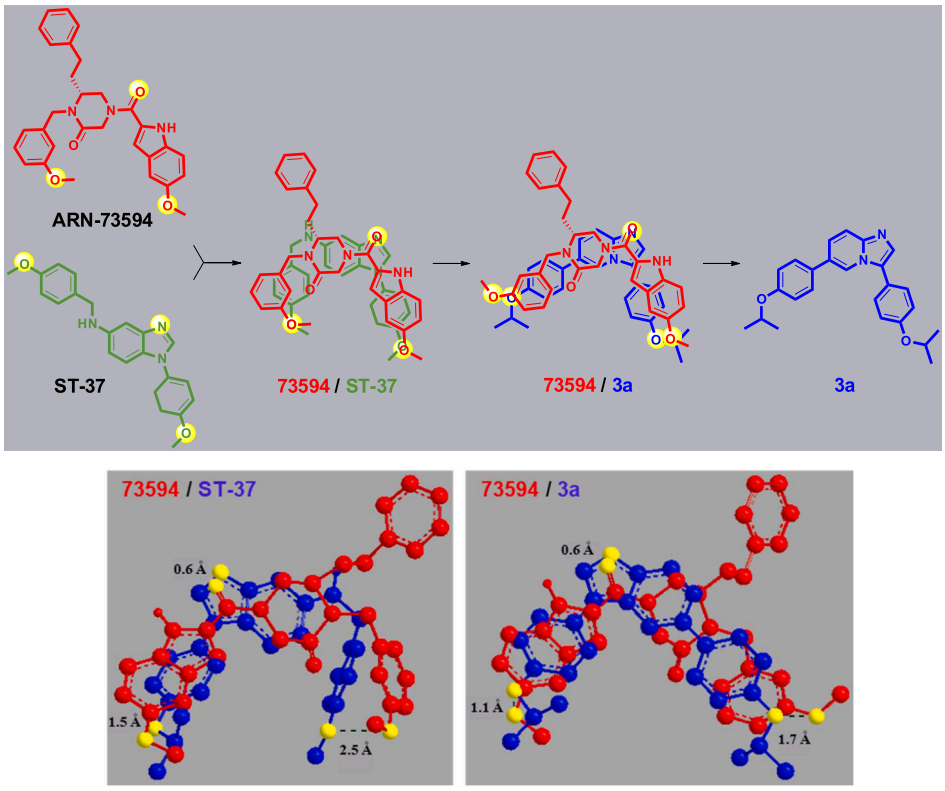

Fig. 1. 2D and 3D minimization overlays of ARN-73594 and ST-37 or **3a**. (Top Panel) 2D overlay illustrating similarities between ARN-73594 and ST-37 or 73594 and the hypothetical 3,6-diaryl imidazopyridine, subsequently synthesized as compound **3a**. Atoms selected for 3D minimization are highlighted in yellow in the structures. (Bottom Left Panel) 3D minimization overlays of ARN-73594 (Red) and ST-37 (Blue) or (Bottom Right Panel) 73594 (Red) and **3a** (Blue). Atoms pairs selected for minimization are shown in yellow. The distance between each set of atom pairs is shown in green.

panel) with the exception of the R^6 group (phenethyl in ARN-73594). When ARN-73594 was subsequently overlaid with new hypothetical core structures we found that for some 3,6-diaryl imidazo[1,2-*a*]pyridines, the critical N^4-acyl carbonyl and imidazopyridine N^1 exhibited similar minimized distances to those of ST-37 while distances between each pair of oxygens in the ethers decreased from 1.5 & 2.5 Ã… to 1.1 & 1.7, respectively (Fig. 1, bottom panel). Among a number of virtual chemical series the imidazo[1,2-*a*]pyridines chemical series was initially prioritized given it's synthetic tractability allowing rapid SAR exploration through a straightforward 2- or 3-step synthetic route starting from commercially available building blocks.

Upon one-step synthesis by a simple Suzuki cross-coupling reaction (Scheme 1), the imidazo[1,2-*a*]pyridine **3a** (Table 1) exhibited sub- to low nanomolar broad spectrum activity against both Old (pLASV) and New World (pMACV and pJUNV) pseudotyped viruses along with improved *in vitro* metabolic stability compared to the 4-acyl-1,6-dialkyl-piperazin-2-one chemical series (e.g., 82% vs. 3% remaining after 1 h in HLM for **3a** vs. ARN-73594). Encouraged by the results, we further explored the SAR of the imidazo[1,2-*a*]pyridines and a number of related heterocyclic cores to identify optimized lead candidate compounds exhibiting low to sub-nanomolar broad-spectrum arenavirus activity and attractive drug-like properties.

Exploration of R^1 and R^2 groups was conducted with combinatorial libraries of imidazo[1,2-*a*]pyridines varying either R^1, while maintaining the 4-isopropoxyphenyl group at R^2 (**3a-s**), or R^2, while retaining the 4-isopropoxyphenyl group at R^1 (**3*t*-z**) as shown in Table 1 using a straightforward 2-step synthetic route shown in Scheme 1. Starting from commercially available 6-bromo-3-iodoimidazo[1,2-*a*]pyridine **1a**, the 4-isopropoxyphenyl group was introduced at R^2 using a corresponding boronic acid under Suzuki cross-coupling conditions to afford intermediate **2a**. A second cross-coupling reaction with a commercial boronic acid or boronic acid pinacol ester $R^1B(OR)_2$ was used to introduce a variety of R^1 groups at the pyridine portion of the molecule to provide a diverse set of compounds **3a-s**. Similarly, starting from commercially

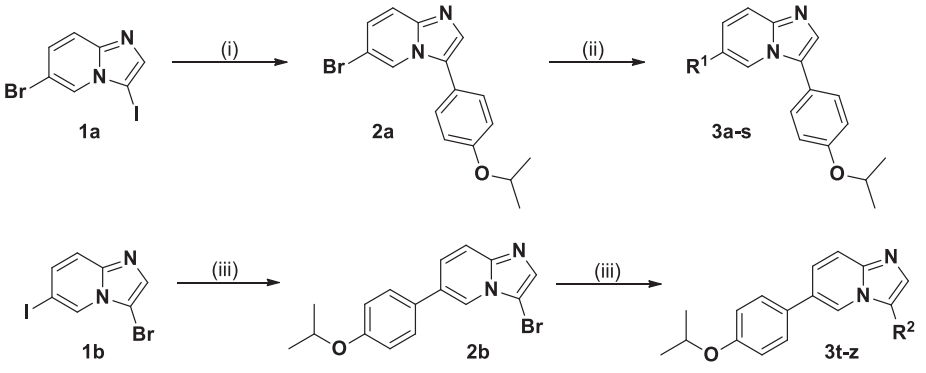

Scheme 1. Reagents and conditions: (i) 4-isopropoxyphenylboronic acid, 7% $Pd(PPh_3)_4$, Na_2CO_3, 1,4-dioxane/H_2O 3:1, degassed with N_2, 90 °C, 5 h (84%); (ii) compound **3a**: 2 eq. 4-isopropoxyphenylboronic acid, 6.5% $Pd(dppf)Cl_2$, Na_2CO_3, 1,4-dioxane/H_2O 3:1, degassed with N_2, 90 °C, 12 h (62%); compounds **3b-s**: $R^1B(OR)_2$, 10% $Pd(dppf)Cl_2$, K_2CO_3, 1,2-dimethoxyethane/H_2O 4:1, degassed with N_2, 90 °C, 5 h (13–54%); (iii) compound **2b**: 4-isopropoxyphenylboronic acid, 10% $Pd(PPh_3)_4$, Na_2CO_3, 1,4-dioxane/H_2O 3:1, degassed with N_2, MW, 90 °C, 15 min (80%); compounds **3*t*-z**: $R^2B(OR)_2$, 10% $Pd(PPh_3)_4$, Na_2CO_3, 1,4-dioxane/H_2O 3:1, degassed with N_2, MW, 90 °C, 15 min (34–56%).

Table 1
SAR exploration of R^1 and R^2 substituents on the imidazo[1,2-*a*]pyridine scaffold. Activity is given as EC_{50} (nM) in the indicated pseudotyped virus assays. Cytotoxicity is given as CC_{50} in Vero cells.

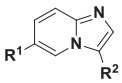

Comp.	R^1	R^2	EC_{50} (nM)*				CC_{50} (μM)
			p-LASV	p-MACV	p-JUNV	p-VSV	
3a	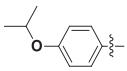	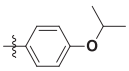	1.03	0.47	0.31	>1000	3.86[a]
3b	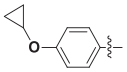	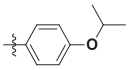	7.25	2.7	1.17	>10,000	6.16[a]
3c	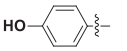	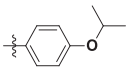	2.69	18.58	7.02	n.d.	10.51[a]
3d	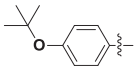	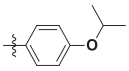	0.67	0.16	0.12	>10,000	3.98[b]
3e	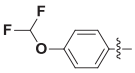	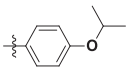	4.35	23.94	4.62	n.d.	4.56[a]
3f	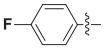	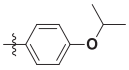	>25	>25	>25	n.d.	4.81[a]
3g	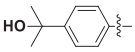	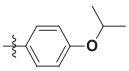	1.11	0.72	0.54	>1,000	12.97[b]
3h	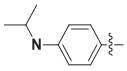	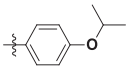	0.56	0.2	0.16	4,530	3.54[b]
3i	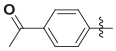	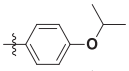	0.29	1.22	0.62	1,880	5.09[a]
3j	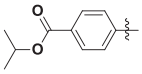	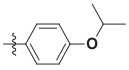	4.98	4.27	0.64	>10,000	3.75[b]
3k	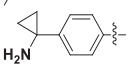	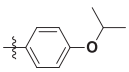	7.97	7.69	2.85	5,060	3.94[a]
3l**	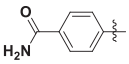	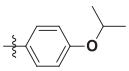	>25	>25	>25	n.d.	n.d.
3m**	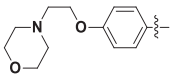	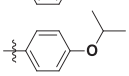	>25	>25	>25	n.d.	n.d.
3n	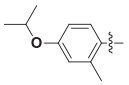	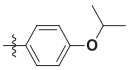	18.13	0.42	0.31	n.d.	3.98[b]
3o	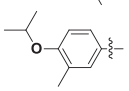	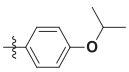	2.35	0.21	0.19	9,860	8.2[b]
3p**	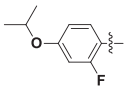	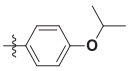	>25	>25	>25	n.d.	n.d.
3q	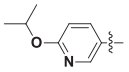	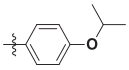	6.07	0.75	1.33	5,060	4.02[a]
3r	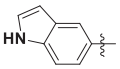	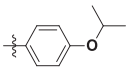	2.03	1.69	1.07	8,120	31.13[a]
3s	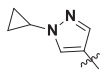	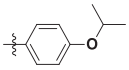	13.36	>25	6.38	n.d.	23.88[b]
3t	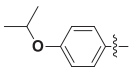		14.46	20.62	11.7	n.d.	6.21[a]
3u			1.35	2.09	0.65	>10,000	8.0[a]
3v			0.40	0.11	0.06	4,840	5.49[a]

(*continued on next page*)

Table 1 (*continued*)

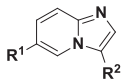

Comp.	R^1	R^2	EC_{50} (nM)*				CC_{50} (μM)
			p-LASV	p-MACV	p-JUNV	p-VSV	
3w	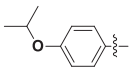	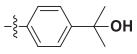	0.85	0.34	0.21	7,390	95.87[b]
3x	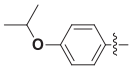	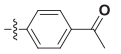	0.67	13.96	1.6	n.d.	8.65[b]
3y	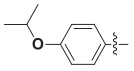	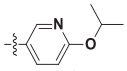	3.61	2.32	0.59	9,950	4.69[a]
3z	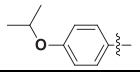	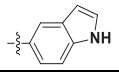	8.41	2.68	0.73	n.d.	>100.00[a]

*Data are average of 2 or more independent experiments, standard deviation <20%, **Data from single experiment, 4 replicates in each experiment.
[a] 7 day cytotoxicity
[b] 5 day cytotoxicity

available 3-bromo-6-iodoimidazo[1,2-*a*]pyridine **1b**, the 4-isopropoxyphenyl group was installed first into the pyridine portion of the molecule to form intermediate **2b**, which then was subjected to a second Suzuki reaction with a variety of commercial boronic acids or boronic acid pinacol esters $R^2B(OR)_2$ introducing diversity at R^2 position in compounds **3*t*-z**.

Analogs with modified R^1 and R^2 substituents were initially evaluated in VSV pseudotyped pLASV, pMACV or pJUNV assays to identify those groups exhibiting low nanomolar broad-spectrum activity.[17] Given the low to sub-nanomolar broad-spectrum potency of an initial imidazo[1,2-*a*]pyridine analog (**3a**, Table 1) we chose an SAR pseudotyped virus activity determination cut-off value of 25 nM. The results from 2D and 3D minimization overlays of ARN-73594 and ST-37 and low to sub-nanomolar broad-spectrum potency of the virtual analog **3a** suggested a preference for *para*-substituted phenyl groups at R^1 and R^2 for potent broad-spectrum activity and we therefore explored a variety of *para*-substituted phenyl groups as well as a number of heterocycles at R^1 and R^2 (Table 1).

Replacing the R^1 isopropoxyphenyl group (**3a**) with the less lipophilic cyclopropoxyphenyl (**3b**) or polar hydroxyphenyl (**3c**) groups decreased activity against each of the pseudotyped viruses while the more lipophilic *tert*-butoxyphenyl group (**3d**) increased potency indicating that potency tracks well with lipophilicity of the *para*-substituted phenyl groups. Replacement of isopropoxy with an oxidation-resistant difluoromethyl group (**3e**) also demonstrated decreased activity while a fluorine group (**3f**) led to an even greater loss in potency (EC_{50} > 25 nM) than the hydroxy group (**3c**). A number of other small 4-substituted R^1 phenyl groups retained low nanomolar broad spectrum activity (**3g-k,** $EC_{50} \leq 8$ nM) with the exception of the polar amide group (**3l**, EC_{50} > 25 nM). However, an attempt to improve solubility by introducing the large polar group morpholinoethoxy led to a dramatic loss of potency (**3m**, EC_{50} > 25 nM). The addition of small substituents such as methyl (**3o**) to the R^1 phenyl meta position was tolerated while similar substitutions at the ortho position decreased the potency against pLASV (**3n**) or each of the pseudotyped viruses (**3p**). Replacing the R^1 phenyl with pyridine or indole heterocyclic groups resulted in compounds retaining low-nanomolar broad spectrum activity (**3q** and **3r**); however, introducing the moderately polar pyrazolyl group led to a substantial loss of activity against pMACV (**3s**, EC_{50} > 25 nM).

Exploring SAR at the right-hand side R^2 aryl group revealed preference for *para*-substitution at the phenyl ring (**3a** vs. **3t**), lipophilic ethers (**3u** and **3v**), and small polar groups (**3w** and **3x**). Substitutions of both pyridine (**3y**) and indole (**3z**) at R^2 retained low-nanomolar broad spectrum activity, albeit with 3 to 8-fold reduced activity against pLASV and pMACV compared to 4-isopropoxyphenyl (**3a**). Compounds of this chemical series exhibited little or no effect when tested against VSV

Table 2
SAR exploration of further group additions to the imidazo[1,2-*a*]pyridine core. Activity is provided as EC_{50} (nM) for the indicated pseudotyped virus assays. Cytotoxicity is shown as CC_{50} in Vero cells (5 days).

Compd.	R^3	R^4	R^5	R^6	EC_{50} (nM)*			CC_{50} (μM)
					p-LASV	p-MACV	p-JUNV	
6	H	Me	H	H	15.48	6.56	4.65	3.81
7	H	H	Me	H	0.42	0.25	0.16	4.71
8	H	H	H	Me	0.32	0.16	0.17	4.19
9	H	H	OMe	H	13.72	3.92	2.38	5.27
10	H	H	CN	H	1.4	0.25	0.22	6.71
11	CN	H	H	H	27.35	>25	3.78	>100.00
12**	C(O)OEt	H	H	H	>25	>25	>25	n.d.
13**	COOH	H	H	H	>25	>25	>25	n.d.
14**	$C(O)NH_2$	H	H	H	>25	>25	>25	49.52

*Data are average of 2 or more independent experiments, standard deviation < 20%, **Data from single experiment, 4 replicates in each experiment.

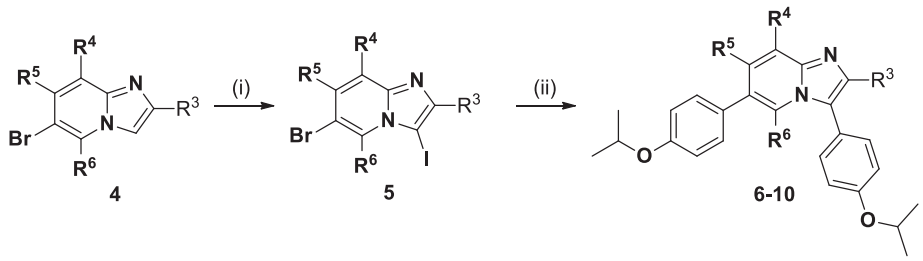

Scheme 2. Reagents and conditions: (i) *N*-Iodosuccinimide, CH_2Cl_2/MeOH 10:1, rt, 2 h (54–77%); (ii) 2 eq. 4-isopropoxyphenylboronic acid, 6.5% Pd(dppf)Cl_2, Na_2CO_3, 1,4-dioxane/H_2O 3:1, degassed with N_2, 90 °C, 12 h (5–71%).

pseudotyped virus expressing the VSV glycoprotein (Table 1, EC_{50}s > 1 μM) defining them as broad spectrum arenavirus entry inhibitors.

In order to confirm that the inhibitory activities observed in pseudotyped virus assays translate to activities against native human hemorrhagic fever arenaviruses, compounds **3a** and **3g** were tested against replicative LASV. EC_{50} values of 16 and 22 nM and SI_{50} values ([CC_{50}]/[EC_{50}]) of 1197 and 920, respectively, were observed, confirming the potent antiviral activity of these imidazo[1,2-*a*]pyridine analogs against pathogenic human hemorrhagic fever arenaviruses.

We subsequently introduced additional substituents into the imidazo[1,2-*a*]pyridine core while retaining 4-isopropoxyphenyl groups at R^1 and R^2 in compounds **6**–**14** (Table 2). Compounds **6**–**10** were prepared through a straightforward 3-step synthetic route by the iodination of the appropriate imidazo[1,2-*a*]pyridine (**4**) with NIS followed by Suzuki coupling of intermediate **5** with 2 eq. of (4-isopropoxyphenyl)boronic acid (Scheme 2). Analogs **11**–**14** were obtained in a similar manner from the appropriate 2-substituted 3,6-dibromoimidazo[1,2-*a*]pyridines (see Supplementary data, Schemes S1 and S2).

Small groups, such as methyl (**7**) and cyano (**10**), were tolerated at R^5 position, with analogs retaining sub to low nanomolar broad spectrum activity while methoxy (**9**) resulted in a decreased pLASV activity (EC_{50} = 13.72 nM). Methyl was also well-tolerated at the R^6 position (**8**) while introducing methyl at R^4 led to a decrease in potency against each of the pseudotyped viruses (**6**). None of the explored polar substituents were tolerated at R^3 as they led to dramatically reduced potencies (**11**–**14**).

We next investigated the replacement of imidazo[1,2-*a*]pyridine with alternative cores by changing nitrogen atoms' position in 5-membered ring and/or adding extra nitrogen atoms into the 5- or 6-membered ring as shown in Table 3. General synthetic routes toward a representative benzimidazole, 7-azabenzimidazole, and benzotriazole analogs are provided in Scheme 3. Benzimidazole and 7-azabenzimidazole analogs **27** and **28**, respectively, were prepared through a 3-step synthetic route. The reaction of nitro compounds **15a,b** with 4-isopropoxyaniline in the presence of K_2CO_3 afforded 2-nitro anilines **16a,b**. One-pot reduction and cyclization[26] of 2-nitro anilines **16a,b** provided benzimidazole or 7-azabenzimidazole intermediates **17a,b**, which were then introduced into Suzuki coupling reaction with 4-isopropoxyphenyl boronic acid to afford benzimidazole **27** and 7-azabenzimidazole **28**. The reaction of nitro compound **15a** with 4-isopropoxyaniline and subsequent reduction of the nitro group followed by the reaction of formed dianiline **18** with nitric acid in the presence of acetic acid and triphenylphosphine afforded 6-bromobenzotriazole **19**. Suzuki coupling of compound **19** with 4-isopropoxyphenyl boronic acid provided benzotriazole **35**.

Imidazo[1,2-*a*]pyrimidine **31** and 1,2,4-triazolo[4,3-*a*]pyridine **34** were prepared through Suzuki coupling of 6-bromoimidazo[1,2-*a*]pyrimidine **20a** or 6-bromo-[1,2,4]triazolo[4,3-*a*]pyridine **20b** with (4-isopropoxyphenyl)boronic acid followed by bromination of the intermediate **21a** or **21b** with *N*-bromosuccinimide and a second Suzuki coupling reaction with the appropriate boronic acid (Scheme 4). General synthetic routes to other analogs from Table 3 are provided in Schemes S3–S10 (Supplementary data).

Replacing the imidazo[1,2-*a*]pyridine core with other imidazopyridine analogs by changing nitrogen atoms' positions led to a dramatic loss of potency against each of the pseudotyped viruses (**23** and **24**, EC_{50}s > 20 nM). Neither indazole (**25** and **26**) retained broad spectrum activity. The benzimidazole demonstrated improved sub-nanomolar activity against every viral species tested (**27**, EC_{50}s ≤ 0.82 nM), while activity of its aza analogs was dependent on the position of the extra nitrogen atom in the 6-membered ring. Thus, 7-azabenzimidazole **28** retained pLASV activity (EC_{50} 0.82 nM) but exhibited decreased pMACV and pJUNV activities, however the analogous 5-azabenzimidazole (**29**) was >20-fold and >30-fold less potent against pLASV and both pMACV and pJUNV, respectively, compared to parent benzimidazole **27**. Purine analog **30** showed a substantial loss of activity against each of the pseudotyped viruses as well. Incorporation of an extra nitrogen atom into 6-membered ring of the imidazo[1,2-*a*]pyridine led to analogs with pLASV and pJUNV activities comparable to the parent compound **3a**, while slightly decreasing pMACV activities (**31** and **33**) with the exception of imidazo[1,2-*a*]pyrazine **32,** which exhibited a 27-fold decrease in pMACV activity (EC_{50} 12.56 nM). Addition of a third nitrogen atom into the 5-membered ring of imidazo[1,2-*a*]pyridine resulted in [1,2,4]triazolo[4,3-*a*]pyridine provided marginal pLASV activity (**34**, EC_{50} 9.6 nM). Benzotriazole **35** demonstrated low- to sub-nanomolar broad spectrum activity comparable to the imidazo[1,2-*a*]pyridine **3a** while the indole compound **36** retained pJUNV but lost both pLASV and pMACV activities. The observed sub- to low nanomolar broad spectrum activity associated with the imidazo[1,2-*a*]pyridine, benzimidazole, 7-azabenzimidazole, benzotriazole, imidazo[1,2-*a*]pyrimidine, and [1,2,4]triazolo[4,3-*a*]pyridine (EC_{50} < 10 nM in every viral species tested) cores indicates the importance of the non-bridgehead nitrogen atom.

Attempts to improve solubility resulted in either decreased or loss of potency and/or broad-spectrum activity (for example, compounds **3c**, **3k**, and **13**) with most of the analogs (Tables 1–3) exhibiting aqueous solubility of 4–35 μM at pH 7.4. We next generated additional analogs (compounds **37**–**40**, Table 4, Schemes S11–S14 (Supplementary data)) containing optimized R^1 and R^2 groups, such as 4-isopropoxyphenyl, 4-(*tert*-butoxy)phenyl), and 4-(2-hydroxypropan-2-yl)phenyl (Table 1) attached to the most active cores identified above (Table 2 and Table 3).

Table 3
SAR exploration of the heterocyclic core. Activity is given as EC_{50} (nM) in the indicated pseudotyped virus assays. Cytotoxicity is given as CC_{50} in Vero cells.

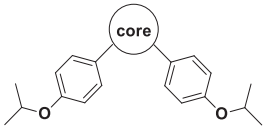

Compd.	Core	EC_{50} (nM)*			CC_{50} (μM)
		p-LASV	p-MACV	p-JUNV	
3a	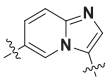	1.03	0.47	0.31	3.86[a]
23	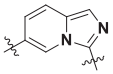	>25	>25	>25	n.d.
24	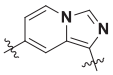	20.92	>25	21.77	7.54[b]
25**	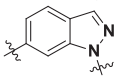	>25	>25	13.98	n.d.
26**	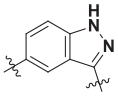	10.5	>25	3.22	5.58[a]
27	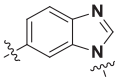	0.82	0.46	0.12	3.09[a]
28	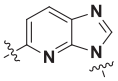	0.82	5.21	3.66	4.14[b]
29	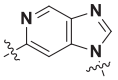	17.75	14.61	4.39	3.99[a]
30**	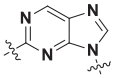	10.71	19.55	3.10	4.68[a]
31	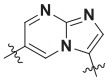	1.24	1.65	0.34	6.23[b]
32	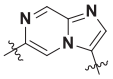	2.95	12.56	2.60	8.51[b]
33	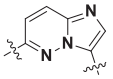	1.50	5.32	0.94	7.72[b]
34	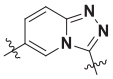	9.6	2.56	1	4.59[b]
35	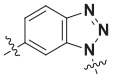	2.82	1.4	0.72	72.96[b]
36	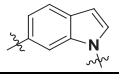	>25	20.64	0.89	n.d.

*Data are average of 2 or more independent experiments, standard deviation <20%, ** Data from single experiment, 4 replicates in each experiment.
[a] 7 day cytotoxicity
[b] 5 day cytotoxicity

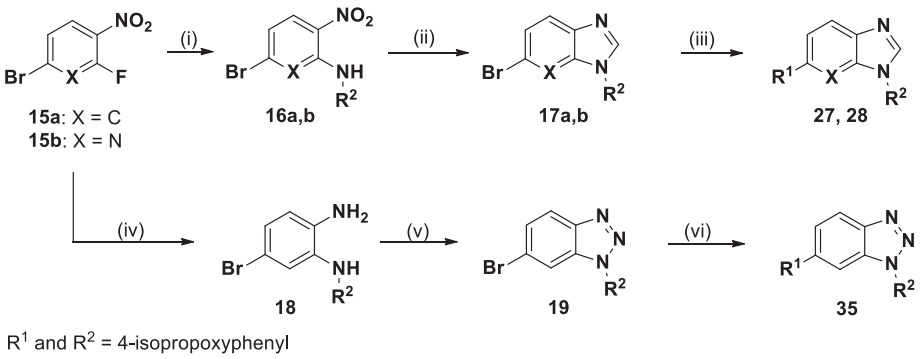

Scheme 3. Reagents and conditions: (i) 4-isopropoxyaniline, K_2CO_3, DMF, 90 °C, 5 h (**16a**, 90%); (ii) iron powder, NH_4Cl, HCOOH, *i*-PrOH, 80 °C, 5 h (**17a**, 68%); **17b**: overall yield for steps (i) and (ii) 12%; (iii) 4-isopropoxyphenylboronic acid, 10% Pd(dppf)Cl_2, K_2CO_3, 1,2-dimethoxyethane/H_2O 4:1, degassed with N_2, 90 °C, 5 h (**27**: 77%, **28**: 9%); (iv) 4-isopropoxyaniline, *i*-PrOH, MW, 120 °C, 30 min, then iron powder, NH_4Cl, EtOH/1,4-dioxane/H_2O 2:2:1, 80 °C 2 h (62%); (v) PPh_3, $NaNO_2$, AcOH, 0 °C, 1 h (95%); (vi) 4-isopropoxyphenylboronic acid, 10% Pd(dppf)Cl_2, K_2CO_3, 1,4-dioxane/H_2O 3:1, degassed with N_2, MW, 120 °C, 30 min (97%).

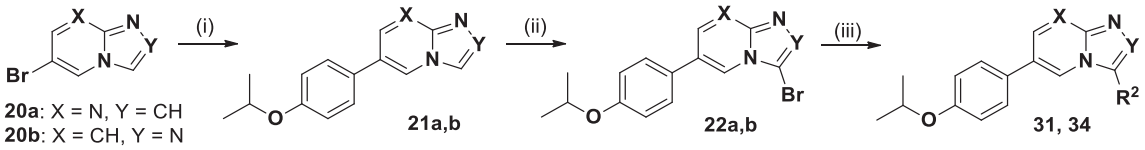

Scheme 4. Reagents and conditions: (i) 4-isopropoxyphenylboronic acid, 10% Pd(dppf)Cl_2, Na_2CO_3, 1,4-dioxane/H_2O 3:1, degassed with N_2, MW, 120 °C, 30 min (**21a**: 78%, **21b**: 65%); (ii) *N*-Bromosuccinimide, CH_2Cl_2/MeOH 10:1, rt, 2 h (**22a**: 77%, **22b**: 56%); (iii) 4-isopropoxyphenylboronic acid, 10% Pd(dppf)Cl_2, Na_2CO_3, 1,4-dioxane/H_2O 3:1, degassed with N_2, MW, 110 °C, 30 min (**31**: 68%, **34**: 65%).

Surprisingly, one of the analogs, i.e. benzimidazole **39**, demonstrated a significantly improved solubility of >100 μM at pH 7.4.

As shown in Table 4, all newly synthesized analogs exhibited sub- to low nanomolar broad spectrum EC_{50} activity against pLASV, pMACV and pJUNV. Similar to the concentration–response curves of earlier analogs, the representative benzotriazole (**35**), imidazopyridine (**37**) and benzimidazole (**38**) compounds exhibit steep cooperative Hill slopes >1 (Fig. 2), which allows for superior antiviral activity for each of the compounds.

For additional SAR comparison and compound prioritization we further assessed initial *in vitro* ADME properties (multi-species microsome stability and hERG K+ channel inhibition) of representative heterocyclic analogs exhibiting EC_{50}s ≤ 10 nM against each of the pseudotyped viruses (Table 4). Thus, the selected compounds were characterized in multispecies liver microsome (MLM) metabolic stability assays including human and the potential efficacy and/or toxicology model species mouse, guinea pig, rat, cynomolgus monkey, and dog. A number of analogs exhibited attractive metabolic stability in all tested species but cynomolgus monkey (**7**, **37**, **38**, **39** and **40**) with the exceptions of benzotriazole analog **35** (>92% parent compound remaining at 60 min in liver microsomes for all tested species) and 7-azabenzimidazole **28** (68% remaining at 60 min in cynomolgus monkey liver microsomes and ≥81% in all other tested species). Interestingly, imidazo[1,2-*a*]pyridine analog **7** bearing a methyl group at R^5 exhibited greater metabolic stability in all species compared to its analog **10** having a cyano group. The other exciting feature of adding methyl group at the R^5 position was the elimination of hERG K+ channel inhibition (**7** vs **3a** and **37** vs **3v**), which was observed in early analogs (**3a** and **3v**) and was a major liability for the cores having a bridgehead nitrogen atom, such as imidazo[1,2-*a*]pyridine (**3a** and **3v**), 1,2,4-triazolo[4,3-*a*]pyridine (**34**) and imidazo[1,2-*a*]pyrimidine (**31**). The lack of hERG K+ channel inhibition for a number of tested compounds suggests favorable potential for cardiac safety.

Prioritized analogs exhibiting EC_{50}s ≤ 4 nM against all tested pseudotyped viruses and having optimal MLM metabolic stability profiles, as well as a lack of hERG K+ channel inhibition (**7**, **35**, **37**, **38**, **39**, and **40**), were selected for further advancement and evaluated for efficacy in replicative LASV plaque assay and LASV and JUNV viral yield reduction (VYR) assays (Table 5). The compounds **7**, **37**, **38**, and **39** demonstrated EC_{50}s of <3.3 nM and SI_{90}s of >3800 in plaque assay format, and were further tested in LASV VYR assay at lower concentrations. All tested compounds exhibited low- to sub-nanomolar activity against both wild-type LASV and JUNV with both EC_{50}s and EC_{90}s in the low- to sub-nanomolar range and SI_{90}s >10,960 for LASV and >1600 for JUNV. These data confirm the antiviral activity of the compounds against replicative LASV and JUNV with potencies that translate well to those found in the pseudotyped pLASV and pJUNV assays.

In addition, four representative compounds (**7**, **37**, **38**, and **39**) were further characterized for inhibition of the main cytochrome P450 (CYP) isoforms (3A4, 1A2, 2B6, 2C9, 2C19, and 2D6) to evaluate the potential for drug-drug interaction liabilities. Tested compounds showed lack of significant inhibition for each of the CYP enzymes (<21% at 20 uM) with the exception of analogs **7** (36% for 2B6) and **38** (44% for 3A4).

In summary, we have discovered a novel chemical series of arenavirus cell entry inhibitors through pharmacophore modeling of two earlier chemical series, targeting the GP2 glycoprotein subunit, that inhibit both pseudotyped and replicative Old and New World arenaviruses with low to sub-nanomolar activity. The prioritized lead compounds, including diphenyl-substituted imidazo[1,2-*a*]pyridines, benzimidazoles, and benzotriazoles, demonstrated attractive metabolic stability in human and nonhuman liver microsomes (except for monkey) and lack inhibition of both hERG K+ channels and major CYP enzymes. Their potent broad-spectrum arenavirus antiviral activity and initial *in vitro* drug-like properties makes them attractive candidates for further

Table 4
SAR of selected cores combined with selected R^1 and R^2 groups. Activities provided are EC_{50} values (nM) in the indicated pseudotyped virus assays. hERG channel assay: % inhibition at 3 μM. Liver microsomal stability data (% remaining after 60 min): H = Human, GP = Guinea Pig, M = Mouse, CM = Cyno Monkey, D = Dog, R = Rat).

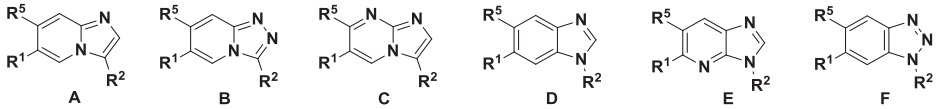

Compd.	Core	R^1	R^2	R^5	EC_{50} (nM)*			hERG % inhibition (3 μM)	Liver microsomal stability
					p-LASV	p-MACV	p-JUNV		
3a	**A**	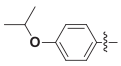	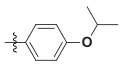	H	1.03	0.47	0.31	89	82 (H), 74 (GP), 100 (M), 53 (CM)
3v	**A**	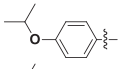	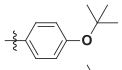	H	0.40	0.11	0.06	48	96 (H), 87 (GP), 85 (M), 28 (CM)
7	**A**	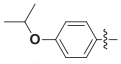	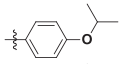	Me	0.42	0.25	0.16	14	100 (H), 78 (GP), 69 (M), 21 (CM), 97 (D), 88 (R)
10	**A**	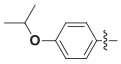	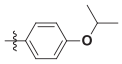	CN	1.4	0.25	0.22	n.d.	88 (H), 55 (GP), 37 (M), 5 (CM), 83 (D), 71 (R)
37	**A**	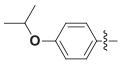	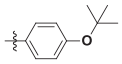	Me	0.68	0.17	0.30	<10	100 (H), 99 (GP), 92 (M), 22 (CM), 100 (D), 100 (R)
34	**B**	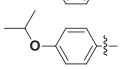	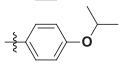	H	9.6	2.56	1.0	57	100 (H), 48 (GP), 0 (CM)
31	**C**	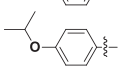	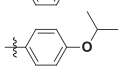	H	1.24	1.65	0.34	37	99 (H), 49 (GP)
27	**D**	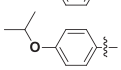	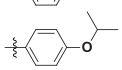	H	0.82	0.46	0.12	30	79 (H), 100 (GP), 78 (M), 37 (CM)
38	**D**	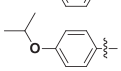	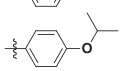	Me	0.65	0.17	0.11	<10	95 (H), 99 (GP), 100 (M), 20 (CM), 100 (D), 100 (R)
39	**D**	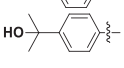	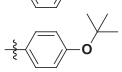	Me	4.0	0.12	1.0	<10	68 (H), 100 (GP), 82 (M), 8 (CM), 100 (D), 93 (R)
28	**E**	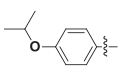	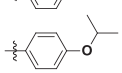	H	0.82	5.21	3.66	<10	100 (H), 81 (GP), 100 (M), 68 (CM), 92 (D), 85 (R)
35	**F**	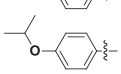	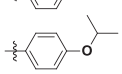	H	2.82	1.4	0.72	17	100 (H), 93 (GP), 99 (M), 98 (CM), 92 (D), 100 (R)
40	**F**	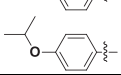	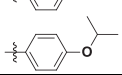	Me	1.05	0.52	0.21	<10	100 (H), 100 (GP), 100 (M), 4.8 (CM), 100 (D), 100 (R)

*Data are average of 2 or more independent experiments (4 replicates in each experiment), standard deviation <20%.

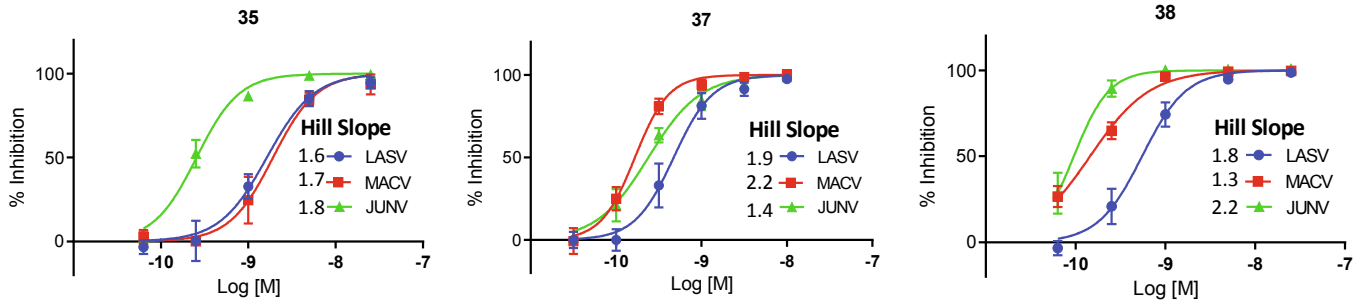

Fig. 2. Concentration–response curves and Hill slopes of representative compounds **35**, **37**, and **38**. Concentration-response curves ± s.d. (4 replicates in each experiment) and Hill slopes of the representative benzotriazole (**35**), imidazopyridine (**37**) and benzimidazole (**38**) compounds for the indicated pseudotyped viruses pLASV, pMACV, and pJUNV are shown.

development of novel small molecule therapeutics to treat Lassa and other arenavirus hemorrhagic fevers. Moreover, the general tractability and straightforward high yielding synthesis of a number of compounds in the chemical series (Supplementary data) offers a solid basis for further process development and cost-effective scale-up, which may help to address potential cost-prohibitive treatment concerns related to the development of therapeutics for emerging viruses in economically challenged geographical settings including Western Africa and some regions of South America.

Table 5
Inhibition of replicative LASV and JUNV. Exemplary compounds and their observed inhibitory activities and selectivity indices (SI) in replicative LASV and JUNV plaque or viral yield reduction (VYR) assays as shown.

Compd.	ARN-number	LASV Plaque Assay EC_{50}/EC_{90} (nM)*	SI_{90}([CC_{50}]/[EC_{90}])	LASV VYR Assay EC_{50}/EC_{90} (nM)	SI_{90} ([CC_{50}]/[EC_{90}])	JUNV VYR Assay EC_{50}/EC_{90} (nM)**	SI_{90} ([CC_{50}]/[EC_{90}])
7	**ARN-74981**	<3.3/<3.3	>3,800	<1.0/<1.0**	>10,960	N/A	N/A
35	**ARN-74982**	N/A	N/A	N/A	N/A	2.9/7.9	3,650
37	**ARN-75039**	<3.3/<3.3	3,900	<0.3/0.87**	>11,481	0.6/1.2	>8,700
38	**ARN-74993**	<3.3/4.2	5,000	1.2/2.1**	14,714	N/A	N/A
39	**ARN-75041**	<3.3/<3.3	>10,000	<0.3/<0.3*	>33,333	0.9/6.2	>1,600
40	**ARN-74994**	N/A	N/A	N/A	N/A	<1.0/2.4	>12,500

*Data are average of 2 independent experiments (3 replicates in each experiment), standard deviation <15%, **Data from single experiment (3 replicates in each experiment), standard deviation <30%.

Declaration of Competing Interest

V.R.G., N.V.S., S.N., E.R.B., G.H. and K.M. are employees of Arisan Therapeutics, which has commercial interests in the development of the chemical series and M.B.P., V.R.G., N.V.S., Y.-J.S., E.R.B., G.H. and K.M. are co-inventors on related patent applications. The other authors declare no competing interests.

Acknowledgement

We gratefully acknowledge the financial support of the National Institutes of Health (Grant R44AI112097 to G.H.). Arisan Therapeutics has utilized the non-clinical and pre-clinical services program offered by the National Institute of Allergy and Infectious Diseases.

Appendix A. Supplementary data

Supplementary data to this article can be found online at https://doi.org/10.1016/j.bmcl.2021.127983.

References

1 Isaacson M. *Clin. Infect. Dis.* 2001;33:1707.
2 Jahrling PB, Geisbert TW. *Nat. Med.* 2004;10:S110.
3 Emonet SF, de la Torre JC, Domingo E, Sevilla N. *Infect. Genet. Evol.* 2009;9:417.
4 Cajimat MNB, Milazzo ML, Rollin PE, et al. *Virus Res.* 2009;140:24.
5 Pontremoli C, Forni D, Sironi M. *Curr. Opin. Virol.* 2018;34:18.
6 Fichet-Calvet E, Rogers DJ. *PLoS Negl. Trop. Dis.* 2009;3, e388.
7 McCormick JB, Fisher-Hoch SP. *Curr. Top. Microbiol. Immunol.* 2002;262:75.
8 Ogbu O, Ajuluchukwu E, Uneke CJ. *J. Vector Dis.* 2007;44:1.
9 Khan SH, Goba A, Chu M, et al. *Antiviral Res.* 2008;78:103.
10 Cummins D, McCormick JB, Bennett D, et al. *JAMA.* 1990;264:2093.
11 Macher AM, Wolfe MS. *Emerg. Infect. Dis.* 2006;12:835.
12 Idemyor VJ. *Natl. Med. Assoc.* 2010;102:1243.
13 Ibekwe TS, Okokhere PO, Asogun D, et al. *Eur. Arch. Otorhinolaryngol.* 2011;268:197.
14 McCormick JB, King IJ, Webb PA, et al. *N. Engl. J. Med.* 1986;314:20.
15 Nomura H, Tanimoto H, Kajiwara E, et al. *J. Gastroenterol. Hepatol.* 2004;19:312.
16 Fuster D, Huertas JA, Gomez G, et al. *Antivir. Ther.* 2005;10:841.
17 Eberhardt KA, Mischlinger J, Jordan S, et al. *Int. J. Infect. Dis.* 2019;87:15.
18 Plewe MB, Whitby LR, Naik S, et al. *Bioorg. Med. Chem. Lett.* 2019;29, 126620.
19 Larson RA, et al. *J. Virol.* 2008;82:10768.
20 Dai D, Burgeson JR, Gharaibeh DN, et al. *Bioorg. Med. Chem. Lett.* 2013;23:744.
21 Burgeson JR, Moore AL, Gharaibeh DN, et al. *Bioorg. Med. Chem. Lett.* 2013;23:750.
22 Albarino CG, Bird BH, Chakrabarti AK, et al. *J. Virol.* 2011;19:10404.
23 Madu IG, Files M, Garaibeh DM, et al. *PLoS Pathog.* 2018;14(12), e1007439.
24 Thomas CJ, Casquilho-Gray HE, York J, et al. *J. Biol. Chem.* 2011;286:6192.
25 Nunberg JH, York J. *Viruses.* 2012;4:83–101.
26 Hanan EJ, Chan BK, Estrada AA, Shore DG, Lyssikatos JP. *Synlett.* 2010;2759.